Available online at www.sciencedirect.com
ScienceDirect
Journal of Catalysis 246 (2007) 413–427
JOURNAL OF CATALYSIS
www.elsevier.com/locate/jcat

Low-temperature NOx reduction with ethanol over Ag/Y: A comparison with Ag/γ-Al_2O_3 and BaNa/Y

Young Hoon Yeom, Meijun Li, Wolfgang M.H. Sachtler, Eric Weitz *

Department of Chemistry and Institute for Catalysis in Energy Processes, Northwestern University, Evanston, IL 60208, USA

Received 28 September 2006; revised 12 December 2006; accepted 17 December 2006

Abstract

A multistep mechanism has been elucidated for the reduction of NOx in the presence of ethanol over silver-exchanged zeolite Y (Ag/Y). Ethanol reacts with O_2 and/or NO_2 to form acetaldehyde at temperatures as low as 200 °C. Surface acetate ions, formed from the oxidation of acetaldehyde, react with NO_2 to yield nitromethane, a critical intermediate in subsequent deNOx chemistry. CN^-, NC^-, and NCO^- are intermediates likely bound to silver ions. Both CN^- and NC^- are stable toward reaction under experimental conditions. A significant difference exists between the catalytic activities of Ag/Y and Ag/γ-Al_2O_3; oxidation of ethanol to acetate at low temperature is significantly faster over Ag/Y than over Ag/γ-Al_2O_3, and both NO_2 and O_2 are effective oxidants over Ag/Y. With Ag/Y, pretreatment with either O_2 or H_2 does not affect the yield of N_2, which approaches 60% and remains constant for at least 5 h, making this catalyst promising for NOx reduction.

Keywords: deNOx; Silver; Zeolite Y; Gamma alumina; Kinetics; Ethanol; Acetate; Acetaldehyde; FTIR; SCR

1. Introduction

Although diesel engines are intrinsically more fuel-efficient than gasoline-powered engines, their exhaust gases are more heavily laden with nitrogen oxides and particulates than those of a comparable gasoline engine whose exhaust has been treated with a standard three-way catalyst [1]. Thus, a societal benefit from the fuel efficiency of diesel engines requires efficient removal of nitrogen oxides (NOx) from diesel exhaust. A goal in NOx removal is to reduce NOx to N_2 with an added reductant and a highly active and selective catalyst.

Ethanol has been successfully used in the selective catalytic reduction (SCR) of NOx on Ag/γ-Al_2O_3, an alumina-supported silver catalyst [2,3]. This system has demonstrated good resistance to both water and sulfur [4], and NOx conversion can exceed 80% in the temperature range of 350–490 °C [5]. Ethanol is a particularly attractive reductant for NOx removal from diesel exhaust because it is environmentally relatively benign and can be blended with diesel fuel using an emulsifying agent [6]. It then can be distilled from this mixture via "on-board" heating. However, the reported working temperature of the Ag/γ-Al_2O_3 catalyst is rather high compared with the typical exhaust gas temperature of light-duty diesel engines of 200–250 °C [7].

In previous work, we found that at 200 °C, the yield of N_2 from NOx reduction by ethanol was ∼55% on Ag/Y, compared with only ∼20% on Ag/γ-Al_2O_3 [8]. More recent studies have explored the reaction mechanism for the SCR of NOx with ethanol over Ag/γ-Al_2O_3 [9–12]. Intermediates including CH_3COO^- [9], $CH_2{=}CHO^-$ [10], NO_3^- [11], and NCO [11,12] have been identified by FTIR spectroscopy. However, remarkably little definitive mechanistic data on the SCR of NOx on Ag/Y are available. It would be particularly interesting to determine how the nature of the intermediates and differences in the reaction mechanism and/or kinetics relate to the differences in catalytic activity of the two supported silver catalysts of interest in this work: Ag/γ-Al_2O_3 and Ag/Y. Understanding the cause of the superior activity of Ag/Y near 200 °C is important, because this low-temperature activity is highly desirable for its removing NOx from diesel exhaust.

The present study used FTIR to identify reaction intermediates in deNOx chemistry occurring over Ag/Y with ethanol

* Corresponding author.
E-mail address: weitz@northwestern.edu (E. Weitz).

0021-9517/$ – see front matter
doi:10.1016/j.jcat.2006.12.013

as an added reductant. These findings form the basis for our discussion of the differences in catalytic activity between Ag/γ-Al_2O_3 and Ag/Y. This comparison is based on both experiments in the present work and previously published work on Ag/γ-Al_2O_3 [9]. We also have considered the effect of the oxidation state of Ag on the catalytic activity of Ag/Y.

2. Experimental

Alumina-supported silver catalysts (Ag/γ-Al_2O_3, containing 4 wt% of Ag) were prepared by impregnating γ-Al_2O_3 (Nanostructures and Amorphous Materials Inc., 99%, 11 nm, 250 $m^2\,g^{-1}$) with an aqueous solution of 0.05 M silver nitrate. The mixture of Ag/γ-Al_2O_3 and silver nitrate solution was stirred for 1 h and kept at 298 K until the water evaporated. The dried sample was then calcined at 773 K for 5 h in an O_2 flow. Ag/Y samples were obtained by threefold wet-ion exchange of Na/Y (Si/Al = 2.5, Aldrich) at ambient temperature with a 0.1 M $AgNO_3$ solution. Before each exchange, the Ag/Y slurry was stirred for 3 h, followed by vacuum filtering, thorough washing with doubly deionized H_2O, and drying in air. This material was then calcined for 5 h at 500 °C in an O_2 flow. ICP analysis revealed that 99.6% of the Na^+ ions were replaced by Ag^+ ions.

In situ FTIR spectra were recorded in transmission mode using a homemade IR cell and a Bio-Rad Excalibur FTS-3000 infrared spectrometer equipped with a HgCdTe (MCT) detector. The infrared cell, described in detail previously [13], consists of a stainless-steel cube with two CaF_2 windows that can be differentially pumped. The tungsten grid that supports the catalysts can be resistively heated. Its temperature is measured by a Chromel–Alumel thermocouple spot-welded to the center of the grid.

Typically, a small brush was used to "paint" ~10 mg of sample, suspended in a water slurry, onto the 1.5 × 1.5 cm tungsten grid, with the temperature held at 353 K. Before each experiment, catalysts were heated in vacuum (2×10^{-6} Torr) for 3 h at 703 K and then cooled to the desired temperature. After this treatment, and before the catalyst was exposed to reactants, a spectrum of the catalyst was recorded and used as the "background."

Unless stated otherwise, each reported spectrum is the result of averaging 70 scans at 4-cm^{-1} resolution under static conditions. A DTGS detector and KBr windows were used in place of a MCT detector and CaF_2 cell windows when it was necessary to obtain spectra of absorptions below ~700 cm^{-1}. Time-resolved spectra were obtained using the "rapid-scan" mode of the FTIR.

Unless otherwise stated, gas mixtures of NO + O_2 (and, in some cases, other gases) were prepared at room temperature and allowed to mix and react for a suitable time (typically overnight) such that the NO, NO_2, and O_2 in the mixture were in equilibrium. This means that in the mixtures used in this study, all of the NO was converted to NO_2. For such mixtures, it was verified that no other (or negligible other) reaction occurred in the gas phase during mixing.

Catalytic tests were carried out in a fixed-bed microflow reactor. In brief, 0.2 g of the powdered Ag/Y catalyst was packed into the quartz reactor. The feed gas composition was regulated by mass-flow controllers (URS-100, UNIT Instruments). Two separate experiments were performed with the flow reactor. First, Ag/Y was exposed to a flowing mixture of He and H_2 in a 1:1 ratio at a flow rate 40 ml min^{-1} at 25 °C. The temperature of the fresh Ag/Y sample was then increased to 300 °C with a temperature ramp of 5 °C min^{-1}. After 3 h at 300 °C, the Ag/Y was cooled to 200 °C and purged with He for 20 min. Ag/Y was then exposed to a flow of 336 ppm EtOH, 500 ppm NO_2, 7% O_2, and 1% water at a flow rate of 200 ml min^{-1}, with He making up the balance of the gas flow. Water vapor was introduced into the reaction system by bubbling He through a H_2O saturator. The composition of the effluent was analyzed on-line with a gas chromatograph (GC) equipped with a thermal conductivity detector (5A column for N_2). Before analyzing the effluent, the mixture was allowed to flow through the system for at least 30 min. The conversion of NO_2 was determined from the formation of N_2 [2]. The Ag/Y catalyst was calcined at 500 °C for 5 h in a mixture of O_2 and He (volumetric ratio = 1/3) at a flow rate of 40 ml min^{-1}. The Ag/Y was then cooled to 200 °C and exposed to a flow of the same composition as described above.

Isocyanic acid (HNCO) was prepared by mixing stearic acid (Aldrich, 98%) with sodium cyanate (Aldrich, 96%) and heating to the melting point of the stearic acid (67–72 °C) [14]. Authentic HCN was prepared by a similar method. Stearic acid was mixed with potassium cyanide (Sigma-Aldrich, 97%). Ethanol (Aldrich, 99.8%), acetic acid (Supelco, 99%), acetic acid-2-^{13}C (Cambridge Isotope, 99% ^{13}C), nitrogen dioxide (Matheson Tri-gas, 99%), nitric oxide-^{15}N (Cambridge Isotope, 98% ^{15}N), and nitromethane (Aldrich, 99%) were used as received. *Caution: Care must be taken in handling and/or synthesizing the toxic gases used in this study.*

3. Results

Elucidation of the reaction mechanism for NO*x* reduction with acetaldehyde over BaNa/Y and with ethanol over Ag/γ-Al_2O_3 has provided a very detailed picture of the chemistry involved in this process. The temperature dependence of the rates of reaction of the intermediates identified in these studies provides insight into why BaNa/Y affects NO*x* reduction at a much lower temperature than Ag/γ-Al_2O_3 [9].

Identifying the intermediates is a crucial step in determining an overall reaction mechanism. FTIR spectroscopy was the principal tool used to determine the intermediates in deNO*x* reactions occurring on Ag/γ-Al_2O_3 and BaNa/Y [9,13] and has been used in this study of Ag/Y. The use of isotopically labeled compounds aids in assigning absorptions to specific intermediates. Experiments also have been performed in which the Ag/Y sample was exposed to H_2 before contact with the NO*x* mixture. The objective of these experiments was to determine whether reduction of Ag, which is expected on exposure of Ag/Y to H_2, affects the performance of the Ag/Y catalyst.

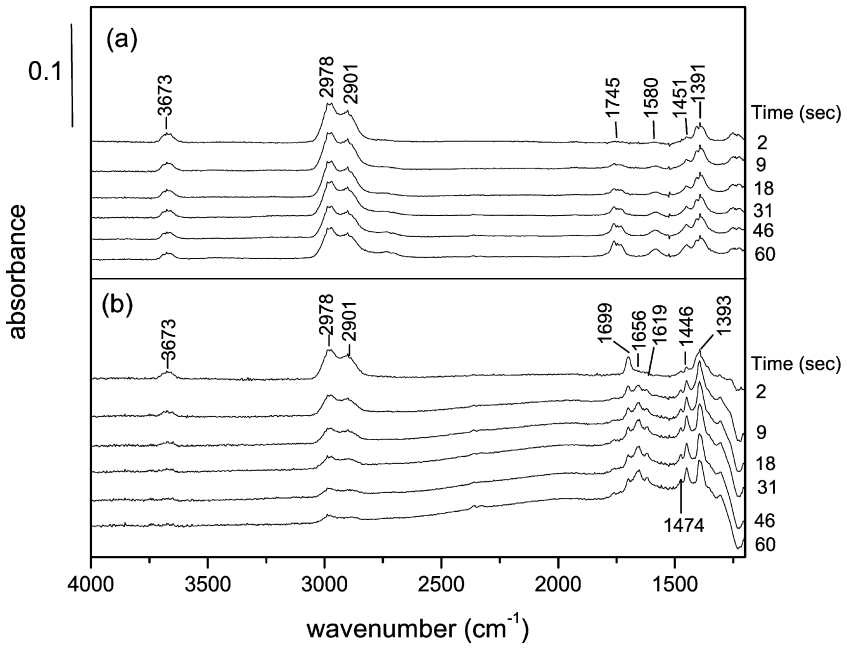

Fig. 1. Time resolved spectra recorded after (a) γ-Ag/Al_2O_3 or (b) Ag/Y was exposed to 100 Torr of a mixture of 3.8 Torr of EtOH + 94.4 Torr of O_2 at 200 °C. The exposure time is indicated for each spectrum.

3.1. Oxidation of ethanol by O_2 on Ag/γ-Al_2O_3 and Ag/Y

On exposing Ag/γ-Al_2O_3 or Ag/Y to a mixture of ethanol + O_2, oxygenated intermediates are observed. In Fig. 1, trace (a), absorption bands at 1391 (CH_3 bending), 2901 (C–H stretch), 2978 (C–H stretch), and 3673 cm^{-1} (O–H stretch) are assigned to ethanol, based on a comparison with the spectrum of authentic ethanol. The absorption at 1745 cm^{-1} is due to gas-phase acetaldehyde, and the band at 1580 cm^{-1} is due to surface acetate [9]. The absorption at 1451 cm^{-1} results from the overlap of the two bands: a bending mode ethanol and the symmetric CO_2^- stretching vibration of surface acetate. The surface acetate is a result of the oxidation of acetaldehyde. The IR bands of acetaldehyde and surface acetate gradually increase in intensity with reaction time.

In trace (b), the absorptions at 2901, 2978, and 3673 cm^{-1} are again due to ethanol. In the top trace, the band at 1699 cm^{-1} first forms and then gradually decreases in intensity, whereas the bands at 1393, 1446, 1474, 1619, and 1656 cm^{-1} gradually increase in intensity. The 1699 cm^{-1} absorption is assigned to acetaldehyde because the same band is observed when Ag/Y is exposed to authentic acetaldehyde. A similar band is also observed when BaNa/Y is exposed to acetaldehyde [13]. The absorption of gas-phase acetaldehyde, centered at 1745 cm^{-1}, seen in the bottom trace is weak compared with the corresponding band in trace (a), because most of the acetaldehyde has been adsorbed. The bands at 1393, 1446, 1474, and 1656 cm^{-1} correspond to absorptions observed when Ag/Y is exposed to authentic crotonaldehyde. The band at 1619 cm^{-1} is best assigned to the overlap of an absorption of crotonaldehyde and surface acetate. These data clearly indicate that some surface acetate is formed by oxidation of acetaldehyde before all of the acetaldehyde reacts to form crotonaldehyde.

Comparing the rate of decrease of ethanol in Fig. 1, traces (a) and (b), demonstrates a much more rapid loss in (b). Thus, ethanol is readily oxidized by O_2 at 200 °C on Ag/Y. Both the relatively higher surface area (~900 vs ~250 $m^2\,g^{-1}$) and the greater quantity of silver (~26 vs ~4 wt%) for Ag/Y versus Ag/γ-Al_2O_3 could contribute to the high rate of oxidation. Details relevant to the rate of ethanol oxidation under different conditions on Ag/γ-Al_2O_3 have been provided in our previous work on this system [9].

3.2. N-containing intermediates in the reaction of NO_2 and ethanol over Ag/γ-Al_2O_3

After exposure of Ag/γ-Al_2O_3 to a mixture of C_2H_5OH + NO + O_2, an intermediate is observed at 2258 cm^{-1} (Fig. 2). In Fig. 2, trace (a), the gas-phase feature centered at 2348 cm^{-1} is due to CO_2, which is present as a result of incomplete purging of the sample compartment of the spectrometer. The absorption at 2258 cm^{-1}, which does not disappear on evacuation of the cell, is due to an adsorbed species. Data for this intermediate were typically acquired at 150 °C, because the intensity of the 2258 cm^{-1} absorption is lower at 200 °C.

^{13}C-labeled EtOH and $^{15}NO_2$ are used to provide additional data for an assignment of this intermediate. In traces (b) and (c), the absorption at 2258 cm^{-1} is shifted to 2197 cm^{-1} on ^{13}C isotopic substitution and to 2244 cm^{-1} on ^{15}N isotopic substitution. As indicated in Table 1, the asymmetric stretching vibration of isocyanate groups (N=C=O) is shifted by ~8–18 cm^{-1} due to substitution of ^{15}N for ^{14}N and by ~56–62 cm^{-1} as a result of ^{13}C labeling. In addition, an isotopic shift of cyanate (M–OCN, M = K, or Na) of 18 cm^{-1} on ^{15}N substitution is seen. However, after substitution of ^{13}C for ^{12}C, adsorbed cyanates usually absorb at significantly lower wavenumbers

(see Table 1) and have different shifts than those seen here. As shown in Table 1, fulminate (another isomer of NCO) absorbs at 2202 cm^{-1} in HgONC with an isotopic shift ($^{14}N \rightarrow {}^{15}N$) of 37 cm^{-1}. Thus, neither fulminate nor cyanate is compatible with either the position or the isotopic shift of the species absorbing at 2258 cm^{-1}. Therefore, the absorption in trace (a) can be confidently assigned to NCO^-, adsorbed on $Ag/\gamma\text{-}Al_2O_3$. Because this IR band is virtually identical with respect to its shape and position on bare $\gamma\text{-}Al_2O_3$, the absorbing species is most likely Al–NCO.

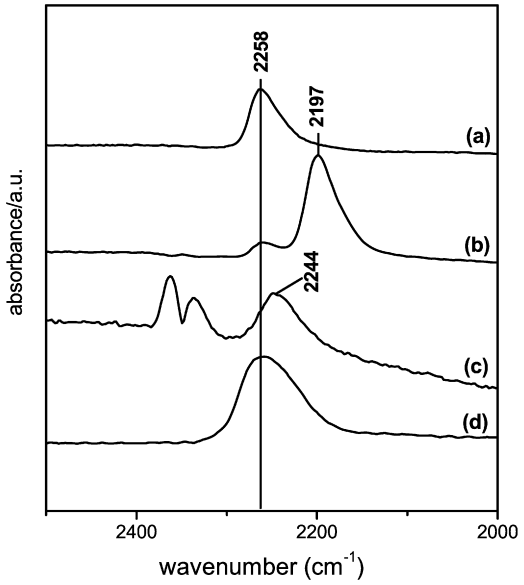

Fig. 2. (a) Spectra recorded after $\gamma\text{-}Ag/Al_2O_3$ was exposed to 100 Torr of a mixture composed of 3.8 Torr EtOH + 3.8 Torr NO_2 + 94.4 Torr O_2 for 1 min at 150 °C. Before spectra were taken, gas-phase species were pumped out. (b) EtOH was replaced by 2-^{13}C EtOH, and (c) NO_2 was replaced by $^{15}NO_2$. (d) Spectrum was taken after $\gamma\text{-}Ag/Al_2O_3$ was exposed to 0.3 Torr of authentic HNCO at 200 °C.

As is evident from Fig. 2, trace (d), one band due to an adsorbed species is observed at 2258 cm^{-1} when $Ag/\gamma - Al_2O_3$ is exposed to HNCO. Gas-phase HCN is also observed. Judging from the positions of the CN and NC absorptions given in Table 1, neither surface NC nor CN is observed under our experimental conditions; these species would be expected to absorb at considerably lower wavenumbers. Interestingly, Bion et al. [11] observed four bands at 2127, 2155, 2255, and 2228 cm^{-1} on exposing Ag/Al_2O_3 to a mixture of EtOH + NO + O_2. Based on our data, the 2255 cm^{-1} absorption observed by Bion is compatible with adsorbed NCO^-. Their observation of additional absorptions is likely due to differences in their catalysts and experimental conditions. Although the positions and the isotopic shift of the NCO absorption do not allow us to uniquely determine whether this species is an anion or neutral, the fact that it is strongly bound to $Ag/\gamma\text{-}Al_2O_3$ suggests that it is an anion, and thus we consider it so in subsequent usage.

Both $N^{12}CO^-$ at 2258 cm^{-1} and $N^{13}CO^-$ at 2197 cm^{-1} are observed when 2-^{13}C EtOH is used as the reductant [Fig. 2, trace (b)]. Clearly, the band at 2197 cm^{-1} in trace (b), due to $N^{13}CO^-$, is much stronger than the band at 2258 cm^{-1} due to $N^{12}CO^-$. This intensity difference demonstrates that most of the carbon atoms in the isocyanate moiety come from the methyl carbon of EtOH. In previous work, a pathway was discussed for the formation of isocyanate from acetaldehyde,

Table 1
Isotopic shift on substituting ^{15}N for ^{14}N and ^{13}C for ^{12}C

	^{14}N and ^{12}C	^{15}N	^{13}C	$^{14}N \rightarrow {}^{15}N$ $\Delta\nu$	$^{12}C \rightarrow {}^{13}C$ $\Delta\nu$	Ref.
HNCO	2266	2258	2206	8	60	
$Ag/\gamma\text{-}Al_2O_3$ + NCO	2258	2244	2197	14	61	This work
SiNCO	2315	2305	2255	10	60	[32]
Pt/Al_2O_3 + NCO	2261	2249	2199	12	62	[32]
	2130	2112	2074	18	56	[32]
MOCN (M = Na, K)	2170	2152		18		
HgONC	2202	2165		37		
HCN	2090	2058		32		
SiCN	2218	2188	2167	30	51	[33]
SiNC	2100	2064	2061	36	39	[33]
AlCN	2144		2097		47	[22]
AlNC	2051		2011		40	[22]

CN (or NC) vibrations in silver compounds

	CN or NC stretch (cm^{-1})	Ref.
AgCN monomer	2171[c]	[34]
AgNC monomer	2075[c]	[34]
AgCN crystal	2164	[35]
Ag–CN in Ag/Y[a]	2166	[36]
Ag/Al_2O_3 + CN[b]	2127 (AgCN)	[12]
	2165 (AlCN)	
	2155 (AlCN)	

[a] Ag^+ ion exchanged zeolite Y.
[b] CN was detected from the reaction EtOH + NO + O_2 on Ag/Al_2O_3.
[c] Calculated.

which is the product of ethanol oxidation [13]; a schematic representation of that pathway is

$$^{13}CH_3CHO + NO_2 \rightarrow\rightarrow H^+ + N^{13}CO^- + CO^2.$$

It is well known that alumina catalyzes ethanol dehydration [12, 15–17]:

$$CH_3CH_2OH \rightarrow CH_2{=}CH_2 + H_2O.$$

To determine whether ethene is formed under our experimental conditions, Ag/γ-Al_2O_3 was exposed to a mixture of 2-^{13}C EtOH + NO_2 + O_2. The results, shown in Fig. 3, indicate a band at 949 cm^{-1} that is assigned to the CH_2 wagging vibration of ethene. This assignment is based on literature data [18] and a comparison with the authentic gas-phase spectrum of ethene obtained in our IR cell. Ethene can then react with NO_2 to produce N-containing intermediates.

Gas-phase H^{13}CN and H^{12}CN are observed at 707 and 719 cm^{-1}, respectively. Interestingly, there is a disparity in intensity, which we address in Section 4. Broad features are present at 680–720 cm^{-1} and 930–950 cm^{-1} in the spectrum obtained at 21 s. These are due to ethyl nitrite formed from the reaction of ethanol and NO_2 [9]. This experiment was conducted at 250 °C, because the ethene concentration was too low to be detected below this temperature. Even though gas-phase hydrogen cyanide is observed, surface cyanide is not detected on Ag/γ-Al_2O_3 under these conditions at 200 or 250 °C. Presumably, the steady-state concentration of surface cyanide is too low to allow detection, due to its rapid reaction with water (vida infra). Two bands at 668 and 649 cm^{-1} are due to the bending modes of $^{12}CO_2$ and $^{13}CO_2$, respectively [18]. There is also a disparity in the intensities of $^{12}CO_2$ and $^{13}CO_2$, which was discussed previously [13].

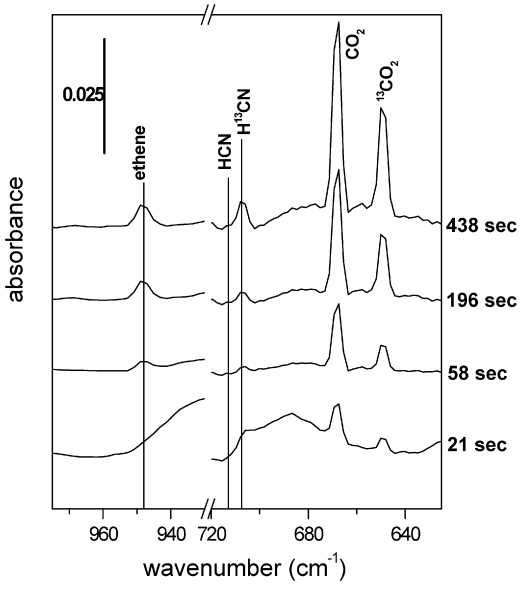

Fig. 3. Gas-phase spectra were recorded at each time frame after Ag/Y was exposed to 70 Torr of a mixture composed of 3.8 Torr 2-^{13}C EtOH + 3.8 Torr NO_2 + 60 Torr of O_2 at 250 °C.

3.3. N-containing products of the reaction of NO_2 and ethanol over Ag/Y

Ethyl nitrite, which is a precursor for acetaldehyde [9], is formed from the reaction of EtOH and NO_2:

$$2NO_2 + EtOH \rightarrow C_2H_5ONO + HNO_3,$$
$$C_2H_5ONO \rightarrow C_2H_5O + NO.$$

The major difference between Ag/γ-Al_2O_3 and Ag/Y is that acetaldehyde is also formed from the direct oxidation of EtOH by O_2 over Ag/Y, at 200 °C, whereas on Ag/γ-Al_2O_3, most of the acetaldehyde is formed from ethyl nitrite at 200 °C. Acetaldehyde can then react with NO_2 to produce nitromethane. It can also be oxidized to surface acetate, which can subsequently react with NO_2 to produce the aci-anion of nitromethane.

Fig. 4 displays changes in the spectra recorded after exposing Ag/Y to a mixture of EtOH + NO_2 + O_2. In trace (a), the absorptions at 1393, 2906, and 2980 cm^{-1} are due to ethanol. The absorption centered at 1616 cm^{-1} is due to gas-phase NO_2, and the absorption at 1699 cm^{-1} is due to adsorbed acetaldehyde. The absorption at 1208 cm^{-1} is likely a zeolite framework vibration. Both the NO_2 and the ethanol absorption rapidly decrease in intensity due to reaction. The 2000–2500 cm^{-1} region is enlarged in the inset. In trace (a) in the insert, absorptions are present at 2090 and 2184 cm^{-1}, and gas-phase CO_2 is seen at 2348 cm^{-1}. The intensity of the absorption band at 2184 cm^{-1} gradually decreases with reaction time and becomes a shoulder of a new absorption that grows in at 2168 cm^{-1}. Although the intensity of the band at 2090 cm^{-1} increases slightly with time, its position does not shift. Neither of the absorptions at 2168 and 2090 cm^{-1} decreases significantly on evacuation, demonstrating strong adsorption of these species on the Ag/Y surface [see trace (h)]. The rapid disappearance of the band at 2184 cm^{-1} with time indicates that this species is reactive. The absorption at 2184 cm^{-1} is due to adsorbed NCO because its position [see trace (e) in Fig. 5] is close to that of NCO observed after exposing Ag/Y to authentic HNCO. Gas-phase HNCO, at 2268 cm^{-1}, is first seen in trace (b), and its intensity gradually decreases as the reaction progresses. Trace (h) shows an additional weak feature at 2236 cm^{-1}; this band is assigned in Figs. 5 and 6. We cannot definitively determine whether the absorption at 2184 cm^{-1} is due to NCO or NCO^-; however, because it is strongly adsorbed on Ag/Y, it is likely NCO^-. The absorption band at 3632 cm^{-1} is assigned to the OH stretching vibration. The same absorption is observed whenever Ag/Y is exposed to authentic HCN. Therefore, this OH absorption is probably the result of dissociation of HCN: HCN → $H^+ + CN^-$. The proton thus formed can attach to a framework oxygen ion.

The experimental data displayed in Fig. 5 provide additional information for the assignment of the three absorptions at 2168, 2090, and 2236 cm^{-1}. These absorptions are stable on evacuation; they form when Ag/Y is exposed to a mixture of EtOH and NO_2. The intensity of the absorption band at 2236 cm^{-1} is dependent on both reaction time and the EtOH/NO_2 ratio. The band intensity increases with time when the EtOH/NO_2 ratio is 1 but is hardly observable when the EtOH/NO_2 ratio

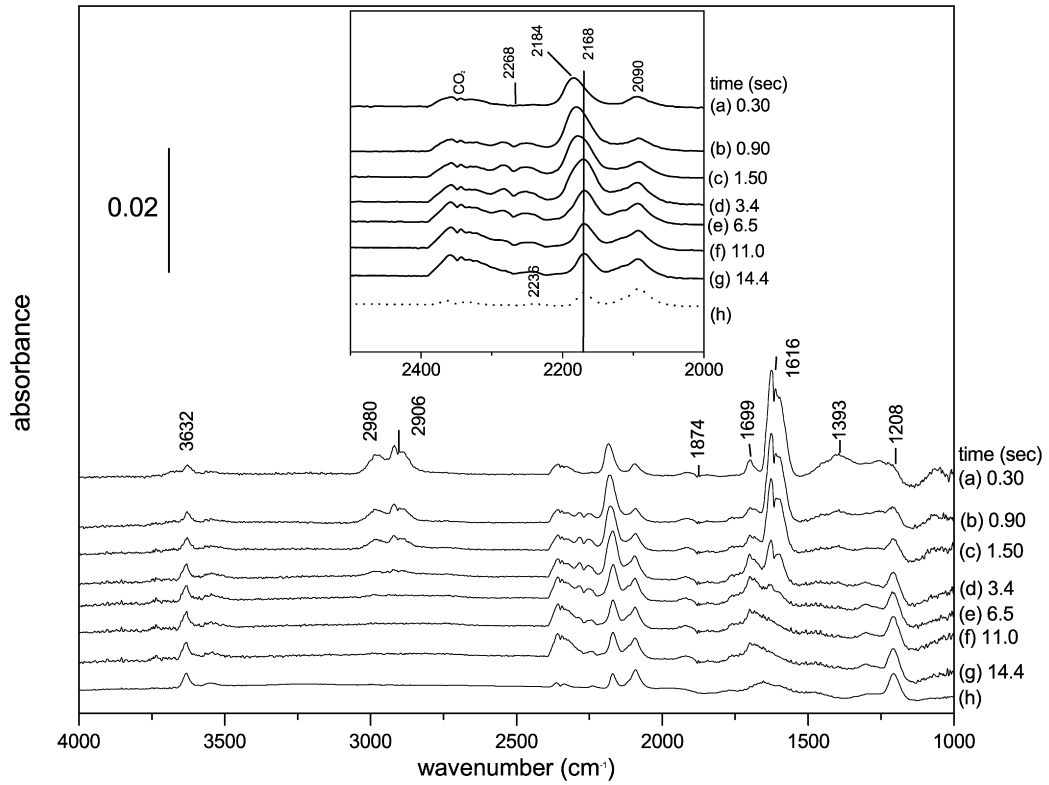

Fig. 4. Time resolved spectra that was recorded after Ag/Y was exposed to 100 Torr of a mixture composed of 3.8 Torr EtOH + 3.8 Torr NO_2 + 92.4 Torr of O_2 at 200 °C, (a)–(g) each spectrum was taken at each indicated time, (h) spectrum was subsequently taken after gas-phase species were pumped off. The insert is a blow up of the ∼2000 to ∼2450 cm^{-1} region.

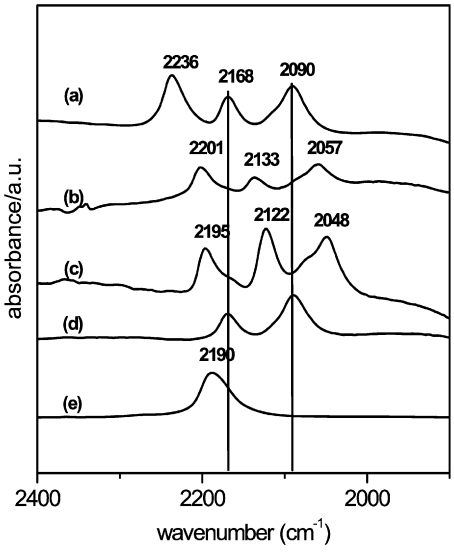

Fig. 5. Spectra were taken after Ag/Y samples were exposed to a mixtures for 10 min at 200 °C. Before spectra were taken, each sample pumped on to remove gas-phase species. The mixtures were (a) 3.8 Torr EtOH + 3.8 Torr NO_2 + 92.4 Torr of O_2, (b) 3.8 Torr EtOH + 3.8 Torr $^{15}NO_2$ + 92.4 Torr of O_2, and (c) 3.8 Torr 2-^{13}C EtOH + 3.8 Torr NO_2 + 92.4 Torr of O_2. Spectra taken after Ag–Y was exposed to authentic (d) 0.15 Torr HCN and (e) 0.15 Torr HNCO.

is 1/3. Although we have not determined the EtOH/NO_2 ratio that optimized the intensity of this absorption, this band becomes weaker when the EtOH/NO_2 ratio is <1.0.

The absorptions at 2168 and 2090 cm^{-1} match well with those that appear when Ag/Y is exposed to authentic HCN; compare traces (a) and (d). These two absorptions, as well as the absorption at 2236 cm^{-1}, shift by the same amount [compare traces (a), (b), and (c)] when either $^{15}NO_2$ or 2-^{13}C EtOH is a reactant. This implies that these three species contain a similar moiety. Based on comparisons of band positions and the isotopic shifts specified in Table 2, the band at 2168 cm^{-1} is assigned to CN^- (cyanide ion), and the band at 2090 cm^{-1} is assigned to NC^- (isocyanide ion). The band at 2236 cm^{-1} does not match any of the bands in traces (b) to (e).

To assign the band at 2236 cm^{-1}, we performed another series of experiments; the results are shown in Fig. 6. When acetaldehyde [trace (b)] and crotonaldehyde [trace (c)] are used as reductants, three bands are observed at positions matching those of the bands in trace (a). Interestingly, when acetic acid is used as the reductant, the absorption at 2236 cm^{-1} is not observed even though the other two absorption bands are observed.

We also exposed Ag/Y to acetonitrile, propanenitrile, pyruvonitrile, and acrylonitrile. The resulting spectra are displayed in traces (e) to (h) of Fig. 6. The only absorption in traces (b) to (h) that matches the 2236 cm^{-1} band is that in trace (g). On exposing Ag/Y to pyruvonitrile [trace (g)], absorptions appear at 2063, 2112, 2168, and 2236 cm^{-1}. This spectrum was obtained after exposing Ag/Y to pyruvonitrile at 200 °C and then cooling to 100 °C. The absorption at 2236 cm^{-1} was not ob-

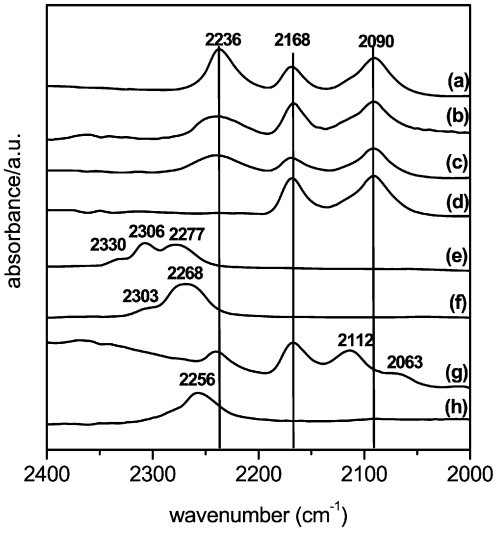

Fig. 6. Spectra were taken after each Ag/Y was exposed to a mixture of (a) 3.8 Torr EtOH + 3.8 Torr NO_2 + 92.4 Torr of O_2, (b) 3.8 Torr acetaldehyde + 3.8 Torr NO_2 + 92.4 Torr of O_2, (c) 3.8 Torr crotonaldehyde + 3.8 Torr NO_2 + 92.4 Torr of O_2, and (d) 3.8 Torr AcOH + 3.8 Torr NO_2 + 92.4 Torr of O_2 for 15 min at 200 °C. Before taking each spectrum, gas-phase species were pumped off. Ag/Y was exposed to (e) 0.4 Torr of acetonitrile, (f) 0.4 Torr propanenitrile, and (h) 0.26 Torr of acrylonitrile at 200 °C. (g) Ag/Y was first exposed to 0.4 Torr of pyruvonitrile at 200 °C and subsequently cooled to 100 °C.

Table 2
Assignments of bands in Fig. 5

Traces	cm^{-1}	Assignments	$^{14}N \rightarrow {}^{15}N$ $\Delta\nu$	$^{12}C \rightarrow {}^{13}C$ $\Delta\nu$
(a)	2090	AgNC, $(NC)_{stretch}$		
	2168	AgCN, $(CN)_{stretch}$		
		–CN[a], $(CN)_{stretch}$		
	2236			
(b)	2057	$Ag^{15}NC$, $(NC)_{stretch}$	31	
	2133	$AgC^{15}N$, $(CN)_{stretch}$	35	
	2201	$–C^{15}N$[a], $(CN)_{stretch}$	35	
(c)	2048	$AgN^{13}C$, $(NC)_{stretch}$		40
	2122	$Ag^{13}CN$, $(CN)_{stretch}$		46
	2195	$–{}^{13}CN$[a], $(CN)_{stretch}$		41
(d)	2090	AgNC, $(NC)_{stretch}$		
	2168	AgCN, $(CN)_{stretch}$		
(e)	2190	AgNCO, $(NCO)_{as\ stretch}$		

[a] –CN=R–C(=O)–C≡N.

served above 100 °C, because this absorption is not thermally stable above 100 °C. The three absorptions at 2168, 2112, and 2063 cm^{-1}, shown in trace (g), are probably the result of a thermal reaction of pyruvonitrile over Ag/Y at 200 °C, because they are not observed when Ag/Y is exposed to pyruvonitrile at 60 °C. When pyruvonitrile is introduced at 60 °C, only a broad absorption at 2228 cm^{-1} is observed, with shoulders at 2220 and 2236 cm^{-1}.

It has been reported that in an Ar matrix, the CN stretching vibration of pyruvonitrile is at 2225 cm^{-1} [19]. However, the band at 2236 cm^{-1} in trace (a) cannot be due to pyruvonitrile monomer, because both its thermal stability and the band position differ from that of authentic pyruvonitrile. We believe that

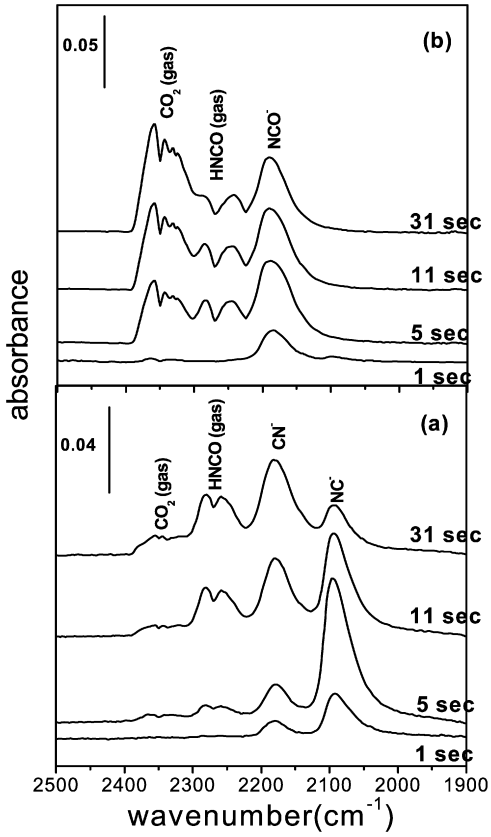

Fig. 7. Time resolved spectra after Ag/Y was exposed (a) to 1 Torr of nitromethane and (b) to 10 Torr of a mixture containing a nitromethane/NO_2 ratio = 1/4. Temperature was 200 °C.

the 2236 cm^{-1} absorption in trace (a) comes from the same absorbing moiety as in pyruvonitrile, namely –(C=O)C≡N. However, this moiety is part of a larger molecule than pyruvonitrile that is strongly bound to the Ag/Y surface. (The possible route for the production of this species is discussed in Section 4.1.) Although s-triazine and melamine have been observed on Co-ZSM-5 during nitromethane decomposition at 553 K [20], neither these molecules nor their derivatives were seen under our reaction conditions.

3.4. Reactions of nitromethane on Ag/Y

In previous work, we reported that NCO^-, but not CN^-, was observed when Ag/γ-Al_2O_3 was exposed to nitromethane (NM) [9]. Absorptions are seen at 719 (not shown here), 2090, 2178, and 2266 cm^{-1} [Fig. 7, trace (a)] on exposing Ag/Y at 200 °C to NM. Gas-phase HCN is readily identified as the absorber at 719 cm^{-1}. The band at 2178 cm^{-1} can be attributed to a combination of two different absorbing species. This is verified by the observation that it splits into two bands on evacuation (not shown here), with the absorption developing at 2164 cm^{-1} due to CN^- and absorption developing at 2190 cm^{-1} due to NCO^-. (These assignments were discussed in the previous section.) Gas-phase CO_2 is also observed at 2348 cm^{-1}. Interestingly, on exposure of Ag/Y to NM, adsorbed isocyanide, with an absorption at 2090 cm^{-1}, is formed before CN^- is observed, and its intensity first increases, then

decreases. On the other hand, both the gas-phase HNCO absorption at 2266 cm^{-1} and the absorption due to both CN^- and NCO^- increase in intensity with reaction time. On a longer time scale, the intensity of HNCO decreases while that of CO_2 increases.

Interestingly, very little CN^- and NC^- is observed when Ag/Y is exposed to a mixture of NM and NO_2 in a 1:4 ratio [Fig. 7, trace (b)]. On the other hand, both NCO^-, at 2190 cm^{-1}, and gas-phase HNCO, at 2266 cm^{-1}, are concurrently observed if NM is in excess relative to NO_2; significant CN^- and NC^- absorptions are also observed. A very weak band due to NC^- is seen in trace (a), where the NM to NO_2 ratio is 1:4. This band is barely observable in subsequent traces because the absorption due to NC^- overlaps with a strong NCO^- absorption. When the sample is evacuated after reaction, absorptions due to NC^- and CN^- become significantly smaller than those shown in trace (a). This demonstrates that NC^- and CN^- are formed under these conditions, but at much lower concentrations than when Ag/Y is exposed to only NM.

Comparing traces (a) and (b) of Fig. 7 demonstrates that the intensity of CO_2 absorption keeps increasing and that its relative intensity is larger than that of the band for HNCO. This indicates that NM reacts more rapidly with NO_2 than it does when in contact only with Ag/Y.

3.5. Thermal stability of surface acetate and nitrate on Ag/Y

On exposure of Ag/Y to acetic acid, strong and broad absorptions in the 1200–1900 cm^{-1} region are seen [Fig. 8, trace (a)]. The absorptions at 1795, 1777, 1727, 1419, and 1293 cm^{-1} [labeled in the top trace in (a)] are due to gas-phase acetic acid. This assignment is based on a comparison with the gas-phase spectrum of authentic acetic acid. Except for the absorptions at 1777 and 1795 cm^{-1}, all acetic acid absorptions overlap with the broad bands of adsorbed acetate. We know of no evidence in the literature, or in our previous studies, to indicate that acetate undergoes a chemical reaction at 50 °C under our experimental conditions. Except for the absorptions due to gas-phase acetic acid, all other absorptions are assigned to surface acetate. As expected, the intensity of absorptions due to gas-phase acetic acid increase with increasing sample temperature, due to the desorption of acetic acid. Even though it is difficult to quantitatively integrate the surface acetate absorptions, due to their overlap with absorptions of gas-phase molecules, the overall intensity change of surface acetate seems small, implying that surface acetate is thermally stable even at 200 °C. Likewise, on Ag/γ-Al_2O_3, surface acetate is stable at 200 °C [9].

On exposing Ag/Y to NO_2, two broad absorptions are observed in the 1200–1500 cm^{-1} region (see the bottom trace in (b) of Fig. 8). As seen with Na/Y and BaNa/Y, these features are in the region where surface nitrates are known to absorb [8]. A broad absorption at 2081 cm^{-1}, with a shoulder at 2178 cm^{-1} (not shown in the figure), is also present at 40 °C. This absorption is due to NO^+ produced from the dissociative heterolytic adsorption of N_2O_4 on the Ag/Y surface [8,13]. N_2O_4 is, of course, in equilibrium with NO_2. NO^+ absorptions have been

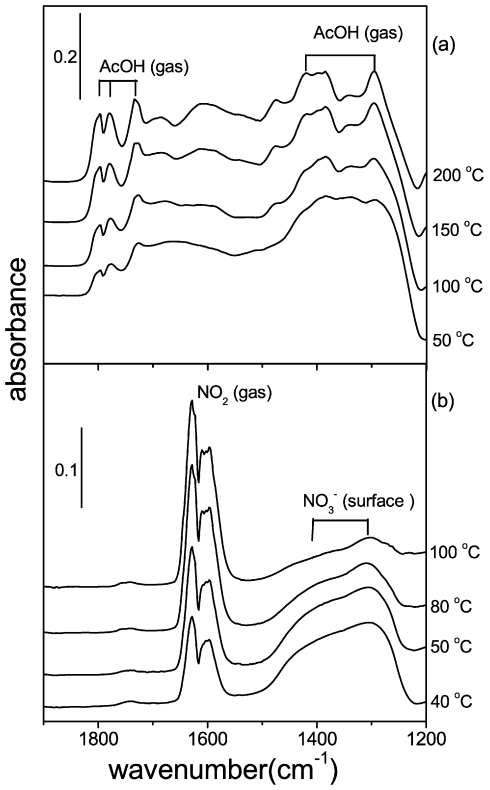

Fig. 8. Temperature of Ag/Y sample was increased after Ag/Y was exposed (a) to 1.2 Torr of acetic acid at 200 °C and (b) to 61.2 Torr of a mixture with an NO_2/O_2 ratio = 1/50.

observed on Na/Y and BaNa/Y, where NO^+ is produced by an analogous reaction [8,13]. With a temperature increase from 40 to 100 °C, gas-phase NO_2 gradually increases in intensity due to desorption, and the integrated area of the surface nitrate band decreases by ∼75%. With a further increase to 200 °C, surface nitrate almost completely disappears. In previous work, we reported on the thermal stability of surface nitrate on Ag/γ-Al_2O_3 [8]. In contrast, with Ag/γ-Al_2O_3, the change in intensity of surface nitrate is small when the temperature is increased from 50 to 100 °C; this indicates that surface nitrate is much more thermally labile on Ag/Y than on Ag/γ-Al_2O_3.

3.6. Reactivity of N-containing surface species

3.6.1. CN^- and NCO^- on Ag/γ-Al_2O_3

Fig. 9, trace (a), shows time-resolved spectra taken after Ag/γ-Al_2O_3 was exposed to authentic HCN. As shown, the intensity of CN^- at 2085 cm^{-1} decreases with exposure time, whereas the intensity of the NCO^- absorption at 2255 cm^{-1} increases. As with NCO^-, by themselves the position and shift of the CN absorption on Ag/γ-Al_2O_3 do not allow us to uniquely identify this moiety as either an anion or a neutral. However, the fact that it is strongly bound to Ag/γ-Al_2O_3 suggest that it is the anion, and thus we refer to it as such.

We subsequently performed the same experiment in the presence of added water [Fig. 9, trace (b)]. Both CN^-, at 2085 cm^{-1}, and NCO^-, at 2258 cm^{-1}, are seen before Ag/γ-Al_2O_3 is exposed to water [top trace in Fig. 9b]. When water

is admitted, the CN^- band vanishes instantaneously. The intensity of the NCO^- absorption at 2258 cm^{-1} also decreases on exposure to water, but at a slower rate than for CN^-. Clearly, CN^- is not simply displaced by water molecules, but is rapidly converted to NCO^- by reacting with water on the Ag/γ-Al_2O_3 surface, based on the following reasoning. The absorption due to CN^- rapidly decreases after the introduction of water and vanishes completely after 0.6 s, due to either rapid displacement or rapid reaction. However, in a separate experiment (not shown here), the CN^- absorption was still observed when Ag/γ-Al_2O_3, which had been pre-exposed to water, was exposed to HCN. In that case, the intensity of the CN^- band rapidly decreased because it reacted with water, and this band was hardly seen after 10 s because CN^- was rapidly converted to NCO^-. The peak position of the NCO^- absorption moved from 2258 to 2250 cm^{-1} as its intensity decreased as a result of this reaction. An analogous shift in the position of the NCO^- absorption was observed on evacuation of the space over a Ag/γ-Al_2O_3 surface on which NCO^- is adsorbed in the absence of added water. Thus, this shift was likely a consequence of changes in the interactions between surface NCO^- species as the surface concentration decreases and/or to interaction with the added water. Therefore, we conclude that the introduction of water leads to rapid loss of CN^- accompanied by a slower loss of NCO^-. Because NCO^- also reacts with water, we interpret this behavior to indicate that CN^- initially reacts with water to form NCO^- on Ag/γ-Al_2O_3. As discussed previously, NCO^- is in equilibrium with HNCO via a reaction with H^+. HNCO can then react with water to form ammonia and CO_2 [13].

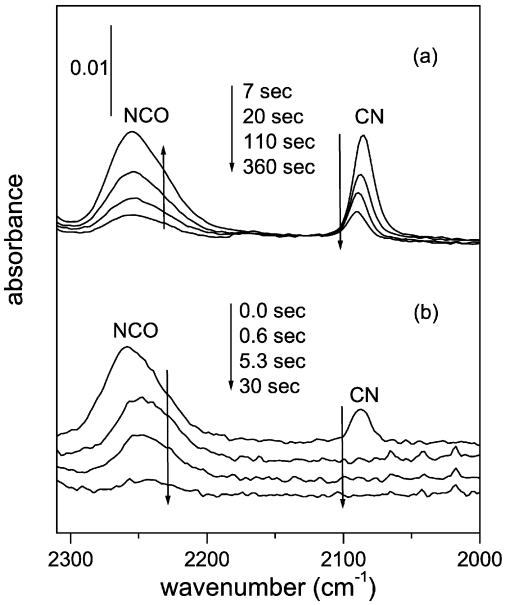

Fig. 9. (a) Time resolved spectra that were registered after Ag/γ-Al_2O_3 was exposed to 0.1 Torr HCN at 200 °C, (b) Ag/γ-Al_2O_3 was first exposed to 0.1 Torr of HCN for 2 min and subsequently exposed to 3 Torr of water.

To obtain data on the reactivity of NCO^- with water without interference from CN^-, Ag/γ-Al_2O_3 was first exposed to authentic HNCO, after which the cell was evacuated to remove any gas-phase HNCO. A strong absorption band at 2255 cm^{-1}, with a shoulder band at 2273 cm^{-1}, is seen in the bottom trace in (a) of Fig. 10. The 2255 cm^{-1} absorption is due to NCO^-, but the absorption at 2273 cm^{-1} could be due to physisorbed HNCO because it is in the appropriate spectral region, and it gradually disappears on evacuation.

After this treatment, water was introduced into the cell. As expected, the NCO^- band at 2255 cm^{-1} and the associated shoulder rapidly decreased in intensity. To demonstrate that this is due to a reaction with water as opposed to displacement by water, separate experiments were performed in which only gas-phase species were monitored. Even at 90 °C, gas-

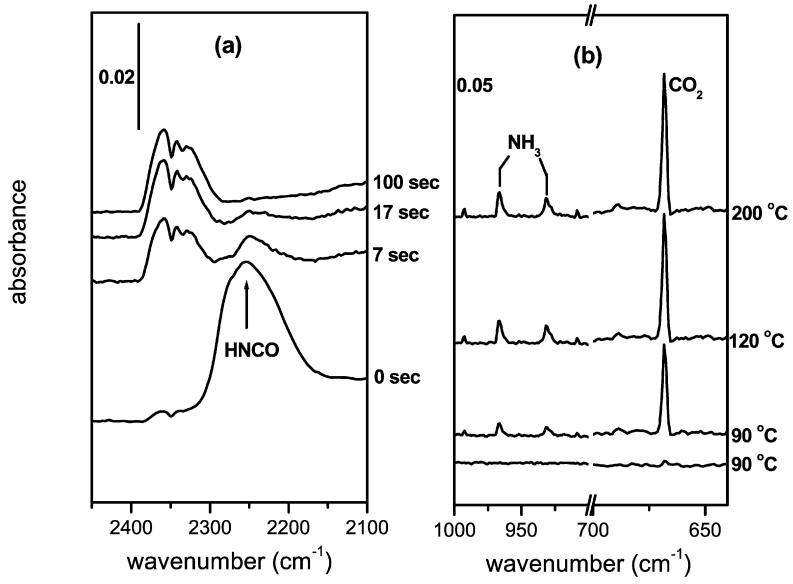

Fig. 10. (a) Ag/γ-Al_2O_3 was first exposed to 0.04 Torr of HNCO at 200 °C and the cell was subsequently evacuated to remove gas-phase species. After the evacuation, the sample was exposed to 10 Torr of water, (b) Ag/γ-Al_2O_3 was first exposed to 0.04 Torr of HNCO at 90 °C and subsequently evacuated. After the evacuation, the sample was exposed to 10 Torr of water and temperature was increased to 200 °C. Temperature ramping was 12 °C min^{-1} from 90 to 120 °C, 30 °C min^{-1} from 120 to 190 °C, 4 °C min^{-1} from 190 to 200 °C.

phase molecules such as CO_2 at 668 cm^{-1} and NH_3 at 931 and 966 cm^{-1} are formed after water is introduced to a catalyst covered with adsorbed NCO^-. The assignments of NH_3 and CO_2 are based on a comparison of gas-phase spectra of authentic CO_2 and NH_3 obtained in our IR cell and literature data [18]. The intensities of these gas-phase absorptions further increase on increasing the temperature from 90 to 120 °C. However, after a temperature rise from 120 to 200 °C, there is no further significant change in the intensity of the absorption of either CO_2 or NH_3. Consistent with this observation, only negligible NCO^- is present on the surface at this point. This clearly demonstrates that NCO^- is very reactive toward water even below 120 °C. To obtain more data on the thermal stability of NCO^- on Ag/γ-Al_2O_3, the temperature of the sample was increased to 300 °C (not shown here). Accompanying this increase in temperature is a gradual decrease in the intensity of the NCO^- absorption, but it does not vanish completely.

As judged by changes in the intensity of NCO^- absorption, NCO^- reacts with added NO_2, but at 200 °C, it is less reactive with NO_2 than with water (not shown here). Bion et al. also studied the reactions of NCO^- with water, NO_2, and O_2 at 300 °C and reported that NCO^- is more reactive with water than with NO_2 or O_2 [12].

On exposing Ag/γ-Al_2O_3 to authentic HCN at 200 °C in the absence of water, absorption bands at 1373, 1448, 1536, and 1603 cm^{-1} are observed (not shown here). The multiplicity of absorptions may be due to HCN which has polymerized on the Ag/γ-Al_2O_3 surface and the absorptions at 1536 and 1603 cm^{-1} would come from the C=N moieties, because these bands shift to lower frequency with $H^{13}CN$. Because CN can be oxidized to NCO^- on Ag/γ-Al_2O_3, cyanuric acid (a trimer of HNCO) could form [20]. However, the bands that are observed do not resemble absorptions obtained when Ag/γ-Al_2O_3 is exposed to authentic cyanuric acid. These absorption are also not observed during the reaction of EtOH + NO_2 + O_2 at 200 °C. The reason for the absence of these absorptions may be due to the rapid reaction of HCN with water, which is produced as part of the reaction sequence. Though the assignment and full interpretation of these absorptions is interesting, it is beyond the scope of this work. Nonetheless, it is clear that the oligomers of HNCO that have been observed by Cant on Co/Y do not form under our experimental conditions on Ag/Y.

3.6.2. N-containing intermediates on Ag/Y

To assess their reactivity on Ag/Y, four N-containing species with absorptions at 2090, 2168, 2184, and 2236 cm^{-1} were generated by exposing Ag/Y to a mixture of EtOH + NO_2 + O_2 at 200 °C. After reaction, the cell was evacuated and the resulting spectrum is shown in trace (a) of Fig. 11. Distinct bands due to R–CN, CN^-, and NC^- are apparent. Under these conditions, an absorption due to NCO^- at 2184 cm^{-1} is observed at early times. The observed bands retain most of their original intensity when the sample temperature is increased to 300 °C. To probe the reactivity of these species, NO_2 was reintroduced. Comparing traces (a) and (c) clearly shows no significant change in intensity of the three absorptions, indicating that these adsorbates do not rapidly react with NO_2. Water was then introduced into the cell, after which the change in intensity of these absorptions was again assessed. Comparing traces (c) and (e) also shows no significant change in intensity of any of the three bands, indicating low reactivity with water under these condi-

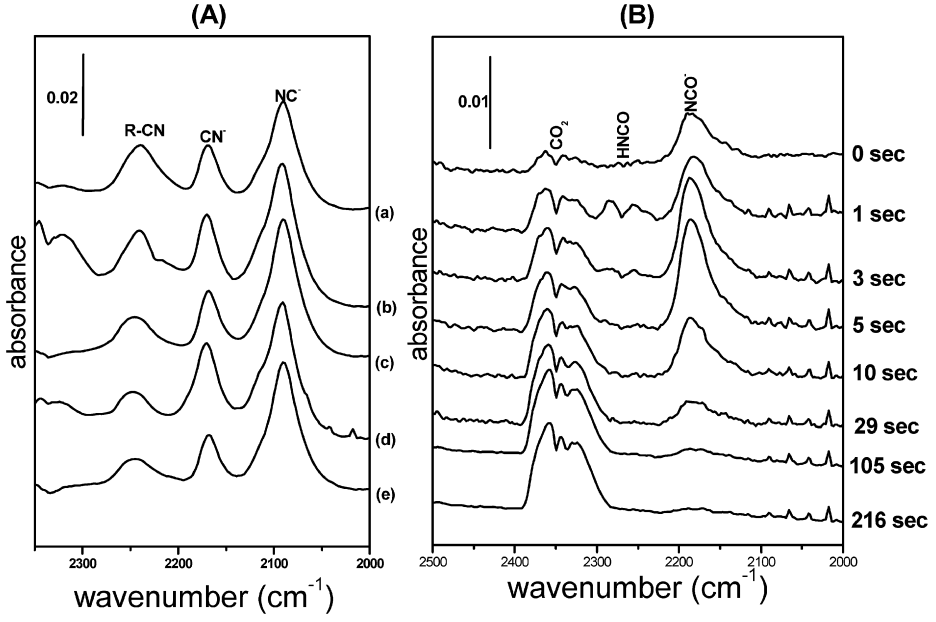

Fig. 11. Panel A: (a) Spectrum was taken after Ag/Y was exposed to a mixture of 3.8 Torr EtOH + 3.8 Torr NO_2 + 92.4 Torr of O_2 for 14 min and cell was subsequently evacuated for 5 min, (b) spectra was taken immediately after subsequent exposure to 4 Torr NO_2, (c) subsequently evacuated after 7 min exposure to 4 Torr NO_2, (d) subsequently exposed to 8 Torr of H_2O, (e) subsequently evacuated after 6 min exposure to 8 Torr of H_2O. Panel B: Ag/Y was exposed to 0.04 Torr of HNCO for 3 min and the IR cell is pumped on for 10 s. Spectra were taken at each time frame immediately after subsequent exposure to 10 Torr of water.

tions. These adsorbates also do not react significantly with NO or O_2 (not shown).

A small shoulder at 2218 cm^{-1} in trace (b) is due to gas-phase N_2O possibly formed from the disproportionation of NO and/or decomposition of ammonium nitrate on Ag/Y [13]. The ammonium nitrate would form from the reaction of ammonia with nitric acid, which is an intermediate in deNOx chemistry [21]:

$$2NO \rightarrow N_2O + \frac{1}{2}O_2$$

and/or

$$NH_4NO_3 \rightarrow N_2O + 2H_2O.$$

It also could be formed from the decomposition of ethyl nitrite, which is a product of the reaction of EtOH and NO_2 [9].

Gas-phase features at 2000–2100 cm^{-1} in trace (d) are due to the added water. To estimate the concentration of NC^- and CN^- in the top trace in (a), a fresh sample of Ag/Y was held under vacuum at 430 °C for 3 h and then cooled to 200 °C. The Ag/Y was subsequently exposed to authentic HCN, with the amount of adsorbed HCN controlled to obtain the desired peak heights. When the peak heights of NC^- and CN^- were comparable to that observed when these molecules are formed from the reaction of EtOH and NO_2, the amount of adsorbed HCN was calculated. This calculation provides estimated concentrations of cyanide and isocyanide produced by the reaction of NO_2 + EtOH. Based on this calculation, the number of adsorbed HCN molecules (equal to the sum of $CN^- + NC^-$) in the top trace in (a) is ∼1 HCN molecule per super cage.

Even though NCO^- is not visible in the traces in (a), this ion is initially observable when Ag/Y is exposed to the indicated mixture. To obtain additional data on the reactivity of NCO^-, Ag/Y was exposed to HNCO, after which the cell was evacuated. The resulting spectra are shown in (b) of Fig. 11. On the introduction of water, the intensity of both gas-phase HNCO and surface NCO^- first increase, then decrease. The initial increase in intensity of these absorptions could be due to displacement of HNCO by water adsorbed on the IR cell wall. Note the 10 s evacuation time for the spectrum shown; evacuating the sample for more than 10 s leads to an intensity of NCO^- that is too weak to observe. If the cell is evacuated after exposure of the Ag/Y to HNCO and then resealed, no increase in the intensity of NCO^- or gas-phase HNCO is evident. The NCO^- band at 2190 cm^{-1} is very small ∼216 s after water is introduced, indicating that NCO^- reacts with water on the Ag/Y surface. Products of this reaction are NH_3 and gas-phase CO_2, which absorbs at 2348 cm^{-1}:

$$HNCO\left(H^+ + NCO^-\right) + H_2O \rightarrow NH_3 + CO_2.$$

The formation of CO_2 demonstrates that NCO^- reacts with water. Ammonia is a co-product of this reaction [21]; however, because ammonia is a much weaker IR absorber than CO_2, it is not observed under the conditions used to generate Fig. 11. The gas-phase features at 2000–2150 cm^{-1} are due to water. The rate of reaction of NCO^- with NO_2 (not shown here) is comparable to that for NCO^- with water.

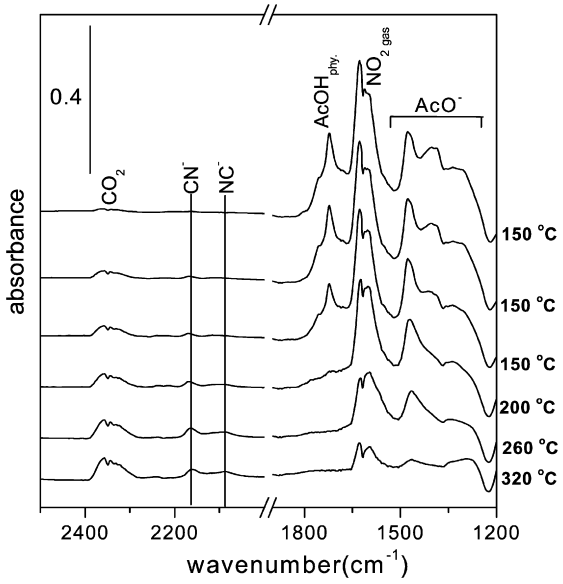

Fig. 12. Ag/Y was pre-exposed to 1.6 Torr of AcOH for 20 min and subsequently evacuated before the introduction of 5.9 Torr of NO_2 (not shown). From top to bottom, the elapsed time for the first three traces is: 1 min, 2 min, and 3.5 min (all at 150 °C). The temperature is then increased from 150 to 320 °C using a ramp of 30 °C min^{-1}.

3.6.3. Reactivity of surface acetate with NO_2 on Ag/Y

As discussed previously [9], surface acetate does not react with NO_2 on Ag/γ-Al_2O_3 at 200 °C. Here we report data on the reactivity of surface acetate with NO_2 on Ag/Y. When Ag/Y is pre-exposed to acetic acid and then exposed to NO_2, N-containing species at 2168 and 2090 cm^{-1} and CO_2 form even at 150 °C (Fig. 12), demonstrating a reaction. On increasing temperature, the rate of the reaction of acetate with NO_2 increases, and physisorbed acetic acid, at 1697 cm^{-1}, disappears. The intensities of surface acetate (at 1240–1500 cm^{-1}) and gas-phase NO_2 also decrease, and gas-phase CO_2 forms. However, the overall rate of reaction of surface acetate is slow at 150–200 °C. Acetate does not react with NO_2 on the Ag/γ-Al_2O_3 surface at 200 °C [9].

To obtain data on the rate of reaction of NO_2 to form N_2 with acetic acid as a reductant, we exposed 200 mg of Ag/Y to a mixture of 1000 ppm acetic acid + 500 ppm NO_2 + 7% O_2 + 1% H_2O at 200 °C at a flow rate of 200 ml min^{-1}. The N_2 GC peak is too small to be integrated, demonstrating that acetic acid is a poor reductant. In contrast, NO_2 conversion to N_2 is ∼56% when ethanol is used as reductant under otherwise identical conditions (Fig. 13). In summary, at 200 °C, surface acetate reacts slowly with NO_2 on Ag/Y but not on Ag/γ-Al_2O_3. Thus, acetic acid is a very poor reductant for conversion of NOx to N_2.

3.7. Effect of pretreatments on of Ag/Y

The effect of pretreating the Ag/Y catalyst on the rate of NO_2 conversion to N_2, was investigated in two separate experiments (Fig. 13). Data acquisition was initiated 30 min after Ag/Y was exposed to the reactants, to ensure that the flow reactor system had stabilized. The data on N_2 yield versus temperature,

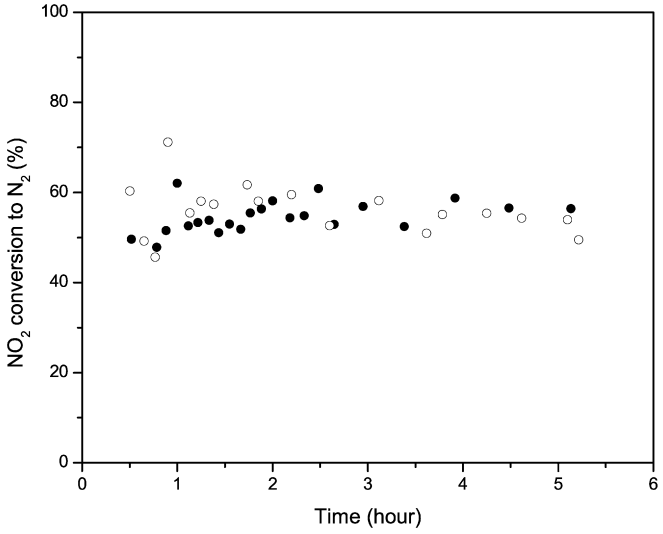

Fig. 13. NO_2 conversion to N_2 over a Ag/Y zeolite catalyst at 200 °C with ethanol as an added reductant. The Ag/Y catalyst was treated with H_2 (○) and with O_2 (●). The experimental details are described in Section 2. (336 ppm EtOH, 500 ppm NO_2, 7% O_2, and 1% H_2O at a flow rate of 200 ml min^{-1}.)

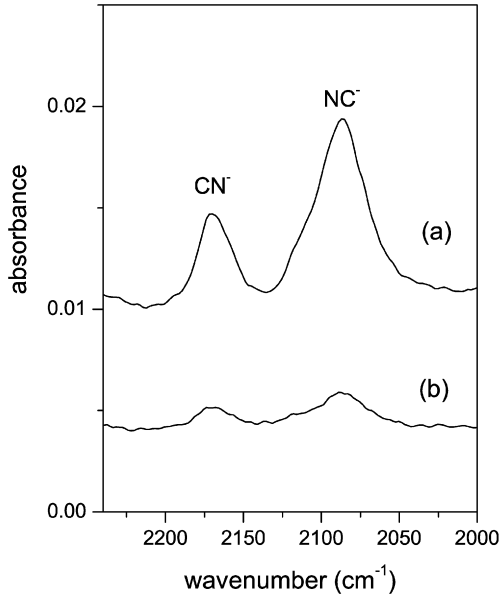

Fig. 14. (a) Before Ag/Y is exposed to 50 mTorr of HCN, it is pretreated with O_2 at 430 °C for 3 h. (b) Before Ag/Y is exposed to 50 mTorr of HCN, Ag/Y was pretreated with H_2 at 430 °C. 10 mg of Ag/Y sample is used in both experiments and gas-phase O_2 or H_2 is pumped way after the pretreatment.

published previously, show that 85% NO_2 is converted to N_2 at ∼300 °C [8]. The rate of the deNO*x* reaction at 200 °C was also monitored after Ag/Y had been pre-exposed to acetic acid; no difference was observed (not shown here). As can be seen in Fig. 13, both catalysts have superior catalytic activity for NO_2 reduction (∼56% N_2 yield) with ethanol at 200 °C, and they do not deactivate during this time period.

To determine whether any change in the intensity of cyanide and isocyanide occurs due to pretreatment, we performed two experiments; the findings are shown in Fig. 14. Interestingly, the peak areas of the absorption of both CN^- and NC^- are approximately five times smaller than those seen when Ag/Y was pretreated by O_2. Even though the peak heights can vary from experiment to experiment, this result indicates that the oxidation state of silver depends on the pretreatment and affects the concentrations of adsorbed CN^- and NC^-. However, there is no measurable difference in the yield for NO_2 conversion to N_2.

4. Discussion

The primary objective of this study is to understand the differences in performance of two silver-containing catalysts, Ag/Y and Ag/γ-Al_2O_3, with regard to the temperature dependence and the yield of deNO*x* reactions with ethanol as a reductant. To do this, we focus on the mechanism and the differences in the nature and reactivity of the intermediates. We start our discussion by outlining the mechanism for deNO*x* chemistry over Ag/γ-Al_2O_3, which has been reported previously [13].

4.1. deNOx mechanism

4.1.1. deNOx reaction mechanism on Ag/γ-Al_2O_3

Two reaction pathways have been identified as participating in deNO*x* chemistry over Ag/γ-Al_2O_3 with ethanol as the reductant. Both of these pathways lead to the formation of nitromethane as a crucial intermediate. The first pathway involves oxidation of ethanol to form acetaldehyde. This mechanism is temperature-dependent, with oxidation by NO_2 dominating at 200 °C and oxidation by O_2 dominating at 300 °C [9]. As discussed in Section 3.2, this reaction competes with the dehydration of ethanol. This dehydration reaction decreases in importance as the concentration of NO_2 (or O_2) increases. The dehydration reaction at 250 °C involves only ∼20% of the ethanol in a mixture of 3.8 Torr EtOH + 3.8 Torr NO_2 + 94.4 Torr O_2. Under typical reaction conditions, for a mixture of EtOH + NO_2 + O_2 at 200 °C, dehydration is of minor importance.

Once acetaldehyde is formed, it readily reacts to form adsorbed acetate ions even in the absence of added O_2. These acetate ions do not significantly react near 200 °C but become reactive near 300 °C. A band due to adsorbed acetaldehyde can be seen at 1706 cm^{-1} at 37 °C (not shown) but is not observed at 200 °C, due to the low surface concentration of acetaldehyde at elevated temperature. The reaction of acetate ions with NO_2 leads to formation of the aci-anion of nitromethane via what has been called the "ionic channel" [9]:

$$CH_3CO_2^- + NO_2 \rightarrow CH_2CO_2^- + HNO_2,$$
$$CH_2CO_2^- + NO_2 \rightarrow CH_2NO_2^- + CO_2$$
$$\overline{CH_3CO_2^- + 2NO_2 \rightarrow CH_2NO_2^- + CO_2 + HNO_2.}$$

The other channel for nitromethane formation involves the formation of methyl radicals as a result of decomposition of acetyl radicals formed from the reaction of acetaldehyde with NO_2. Reaction of methyl radicals with NO_2 then leads to nitromethane. This channel "bypasses" surface acetate involved in the ionic channel, which displays little reactivity below 300 °C. CO is a co-product of the dissociation of acetyl radicals to form methyl radicals and thus serves as a marker for this

"radical channel":

$$CH_3CO^{\bullet} \rightarrow CH_3^{\bullet} + CO.$$

However, no CO is observed over Ag/γ-Al_2O_3 at 200 °C indicating that acetyl radicals are not efficiently formed at that temperature. Thus, neither pathway leads to significant NO*x* reduction at temperatures substantially below 300 °C: For the ionic path, reaction of acetate is rate-limiting, whereas formation of acetyl radicals and/or the reaction of methyl radicals with NO_2 appears to be the rate-limiting step(s) for the radical pathway.

4.1.2. deNOx mechanism on Ag/Y

Ethanol is readily oxidized to acetaldehyde (AA) by O_2 over Ag/Y at 200 °C. Once acetaldehyde (AA) is formed, it reacts with both NO_2 and O_2 to form surface acetate. This reaction sequence is schematically summarized as

$$EtOH + NO_2 \text{ (or } O_2) \rightarrow AA,$$
$$AA + NO_2 \text{ (or } O_2) \rightarrow \text{acetic acid.}$$

Acetaldehyde can react to form crotonaldehyde on Ag/Y, but this reaction is effectively suppressed in the presence of typical concentrations of NO*x*; under these conditions, surface acetate prevails.

Surface acetate will react with NO_2 to form nitromethane. This reaction, although slow at 200 °C, takes place on Ag/Y, and its rate increases as the temperature approaches 300 °C.

Various N-containing intermediates can form over Ag/Y, as discussed in Section 3.3. An open question is whether these intermediates accumulate during the reaction and poison the catalyst. Three of the four N-containing intermediates observed on Ag/Y—NCO^-, NC^-, and CN^-—are products of the reaction of nitromethane. The fourth, R–CN, is formed from the reaction of aldol condensation products with NO_2. Isocyanate (NCO^-) does not "poison" the Ag/Y surface because it reacts readily with water:

$$\text{–Al–OH} + \text{OCN–Al–} + H_2O \rightarrow \text{–Al–O–Al–} + NH_3 + CO_2.$$

Isocyanate ions also react with NO_2, but at 200 °C, this reaction is slower than that of NCO^- with water. The other intermediates, CN^-, NC^-, and RCN, could "poison" the Ag/Y catalyst because they do not react swiftly with H_2O, NO_2, or O_2.

With the exception of R–CN, the mechanism of formation of these N-containing intermediates from the reaction of ethanol and NO_2 is virtually identical on Ag/Y and Ag/γ-Al_2O_3. The immediate precursor for the N-containing species is nitromethane (NM). Interestingly, when NM decomposes on Ag/Y, NC^- (the initial N-containing intermediate) converts to CN^-.

The cyanide and isocyanide ions are likely in equilibrium, because their energies are expected to be similar. Calculations show an energy difference between MgCN and MgNC of 1.5 and 5.5 kcal mol^{-1} between AlCN and AlNC [22]. As expected, the CN stretching frequencies of MCN (M = 13 different metals) are between 2125 and 2175 cm^{-1}, and those of MNC are between 2045 and 2055 cm^{-1} [22].

The mechanism for forming R–CN differs from that for forming the other N-containing species on Ag/Y. When acetic acid is the reductant, no R–CN intermediate is observed. This molecule is seen when EtOH, AA, or crotonaldehyde is used as the reductant. R–CN is thermally stable and relatively nonreactive under experimental conditions, even at 300 °C. When ethanol is the reductant, it first must be oxidized to acetaldehyde on Ag/Y. Aldol condensation occurs with acetaldehyde on Ag/Y in the presence of insufficient NO_2 and O_2 to stoichiometrically react with acetaldehyde. In excess NO_2 and O_2, acetaldehyde preferentially reacts with these molecules to give surface acetate (and acetyl radicals), whereas the aldol condensation becomes negligible. As expected from this description, the intensity of the R–CN absorption depends on the EtOH/NO_2 ratio. If there is excess NO_2, then very little, if any, R–CN is present.

The stable R–CN molecule that can form on Ag/Y cannot be pyruvonitrile, because the positions of IR absorption bands of pyruvonitrile differ from those observed here, and pyruvonitrile reacts on Ag/Y at 200 °C. Instead, the absorption at 2236 cm^{-1} is likely due to a molecule that has a –(CO)–CN functional group. This R–CN molecule on Ag/Y also appears to have a longer chain length than pyruvonitrile. Scheme 1 shows a plausible schematic mechanism for the production of this R–CN molecule.

No R–CN is observed on Ag/γ-Al_2O_3. This can be explained by the fact that neither crotonaldehyde nor any other product of aldol condensation is formed on the Ag/γ-Al_2O_3 surface. When Ag/γ-Al_2O_3 is exposed to AA or AA + NO_2 acetaldehyde is efficiently oxidized to acetate [9].

It is known that CN^- on Ag/γ-Al_2O_3 and both NC^- and CN^- on Ag/Y are precursors for NH_3 in NO_2 reduction. However, we do not believe that these ions are major precursors for NH_3 in these systems. Although NC^- and CN^- are products of NM decomposition [23], under the present experimental conditions, the reaction of NM with NO_2 is more rapid than NM decomposition. Thus, NM will preferentially react with NO_2 to produce dinitromethane, which is expected to be in equilibrium with its aci-anion, a precursor for the aci-anion of dinitromethane:

$$NO_2 + CH_2\text{–}NO_2^- \rightarrow O_2N\text{–}CH_2\text{–}NO_2^-.$$

This reaction has been discussed in detail previously [13]. The dinitromethane anion subsequently decomposes to NCO^-; however, if the concentration of NO_2 is low, then some of the NM might decompose to $HCN + H_2O + \frac{1}{2}O_2$.

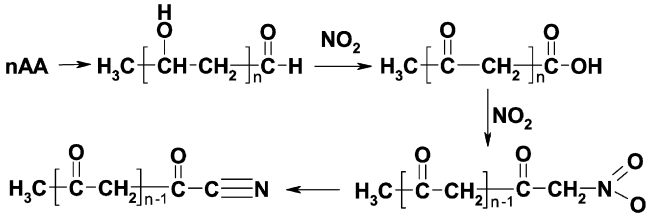

Scheme 1.

In summary, oxidation of ethanol to acetate is not the rate-determining step under the present experimental conditions; in fact, surface acetate is readily formed in either the presence or the absence of N-containing surface species. When the surface is saturated with acetate, the reaction of acetate with NO_2 is very slow at 200 °C. A slow reaction of surface acetate on an acetate-saturated surface was also observed on BaNa/Y [13]. No deactivation of the NO_2 reduction process by EtOH is observed. It provides an N_2 yield of ∼56%.

Surface nitrates do not poison the Ag/Y catalyst, because they are only weakly bound to the surface. On the other hand, if the surface is saturated with acetate, then the reaction with NO_2 is slow even at temperatures where the reaction is efficient at lower concentrations of surface acetate.

4.2. The effect of reducing Ag with H_2

The oxidation state of silver and the form in which it is present in a zeolite can change during the course of a reaction and/or as a result of pretreatment with H_2 or O_2. Hattori's group reported that the addition of hydrogen increases the activity of Ag-zeolites for the selective reduction of NO by hydrocarbons [24]. They attributed this effect to the formation of $Ag_n^{\delta+}$ clusters due to partial reduction and agglomeration of Ag^+ [25]. It also has been reported that the conversion of NO to N_2 with CH_4 over a Ag, H/ZSM-5 increases with the amount of reduced silver [26]. During the SCR reaction over this catalyst, Ag^0 is gradually oxidized by O_2 in the feed, resulting in gradually decreasing NO conversion to N_2 with time on stream.

In flow reactor experiments, we compared the N_2 yield with or without a catalyst pretreatment in a flow of H_2 at 300 °C. Within the limits of experimental error, the yields of N_2 are the same. Under our experimental conditions, both reductants (EtOH) and oxidants (O_2 and NO_2) are present, and the oxidation state and morphology of the silver can change. For example, some of the Ag^+ ions in Ag/Y pretreated with O_2 can be reduced by EtOH and form Ag clusters, whereas some of the metallic silver in Ag/Y pretreated with H_2 may be oxidized to Ag^+ and/or cationic clusters [27].

As discussed previously, roughly one Ag^+ ion per supercage is accessible to CN^- and NC^-. Because our data indicate that Ag is fully exchanged, the remaining silver cations are likely located in sites inaccessible to HCN or form neutral silver clusters and/or cationic clusters. Such clusters may be major contributors to NO_2 reduction. Even though the role of silver in NOx reduction on Ag/γ-Al_2O_3 remains a matter of debate, it is generally accepted that silver cations coexist with other silver species [28–31]. Hattori et al. proposed that dispersed silver clusters are responsible for NOx reduction on Ag-zeolites [25]. Ag^+ ions are probably not important active sites for NO_2 reduction with EtOH, however, because CN^- and NC^-, are strongly bound to these cations.

Finally, we discuss two observations that suggest that CN^- and NC^-, are bound to Ag^+ ions. First, NC^- and CN^- ions are much more reactive on BaNa/Y and Na/Y zeolites than on Ag/Y. Second, on Ag/Y the intensity of CN^- and NC^- absorption depends on the oxidation state of silver. Both CN^- and NC^- absorptions become very weak after exposure of Ag/Y to H_2 (Section 3.7) but remain strong after exposure of Ag/Y to O_2. Stable CN^- and NC^- moieties are not seen on Ag/γ-Al_2O_3, because these species are very reactive with H_2O. The superior reactivity of CN^- and NC^- on Ag/γ-Al_2O_3 as compared to Ag/Y may be due to differing metal–support interactions of the silver ion on these supports. CN^- and NC^- are expected to be bound to Ag^+ ions located in site II of Ag/Y, because such ions are probably unable to access cations in the β-cage with a window diameter of 2.8 Å.

5. Conclusions

The mechanism for deNOx chemistry over Ag/Y with ethanol as an added reductant is qualitatively similar to that over Ag/γ-Al_2O_3, but there are some important differences in the reactivity of some intermediates. As has been observed for Ag/γ-Al_2O_3, in the presence of a mixture of NO_2 and O_2 ethanol is converted to acetaldehyde over Ag/Y. However, unlike with Ag/γ-Al_2O_3, under experimental conditions, acetaldehyde is formed mainly as a result of oxidation of ethanol by O_2. Over Ag/Y, oxidation with O_2 successfully competes with the oxidation of ethanol by NO_2 at a lower temperature than has been observed with Ag/γ-Al_2O_3.

Chemistry that occurs subsequent to formation of acetaldehyde parallels the major features of the deNOx chemistry reported for acetaldehyde as an added reductant over BaNa/Y. Acetaldehyde interacts with Ag/Y to form surface acetate. This surface acetate reacts with NO_2 to form the aci-anion of nitromethane, which is in equilibrium with nitromethane. Nitromethane can react with another NO_2 molecule to form a dinitromethane molecule, which decomposes to HNCO. These steps are depicted in Scheme 2.

The chemistry after HNCO formation is well established and involves hydrolysis of HNCO to form NH_3 and the reaction of NH_3 with nitrous acid (HONO) to form ammonium nitrite. Ammonium nitrite is thermally unstable above 100 °C and decomposes to form H_2O and N_2.

Although the mechanism for deNOx chemistry on Ag/Y is qualitatively similar to what is observed on Ag/γ-Al_2O_3, the yield of N_2 is much higher with Ag/Y at temperatures below 300 °C. This is due essentially to the rate of reaction of surface acetate, which is much faster on Ag/Y than on Ag/γ-Al_2O_3, where virtually no reaction of surface acetate is observed below about 300 °C. However, this reaction appears to be the rate-

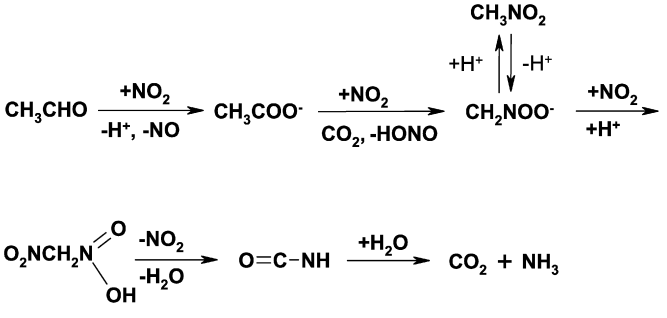

Scheme 2.

Table 3
Assignments of bands in Fig. 6

Traces	cm^{-1}	Assignments
(a)–(d)	2090	AgNC, $(NC)_{stretch}$
	2168	AgCN, $(CN)_{stretch}$
	2236	–CN[a], $(CN)_{stretch}$
(e)	2277, 2306, 2330	CH_3CN, $(CN)_{stretch}$
(f)	2268, 2303	CH_3CH_2CN, $(CN)_{stretch}$
(g)	2063, 2112, 2168, 2236	–CN[b], $(CN)_{stretch}$
(h)	2256	CH_2=CH–CN, $(CN)_{stretch}$

[a] –CN=R–C(=O)–C≡N.

[b] –CN=H_3C–C(=O)–C≡N.

limiting step in deNOx chemistry with ethanol or acetaldehyde as a reductant over both catalysts.

There is no significant effect on the yield of N_2 as a result of pretreating Ag/Y with either O_2 or H_2, despite the fact that it is generally accepted that such pretreatments oxidize metallic silver to Ag^+ and reduce Ag^+ to Ag^0, respectively. Oxidation in the flowing reaction stream may rapidly reverse any reduction occurring due to pretreatment with H_2. Thus, in the steady state, the reacting surface may be oxidized independent of the pretreatment used. Evidence also indicates that both NC^- and CN^- are bound to Ag^+ on Ag/Y.

Finally, the yield of N_2 does not change significantly over time when Ag/Y is exposed to a flowing mixture of EtOH/NO_2/O_2/H_2O (336 ppm EtOH, 500 ppm NO_2, 7% O_2, and 1% water at a flow rate of 200 ml min^{-1}). Under these conditions, as shown in Fig. 13, the yield of N_2 can approach ∼60%, making this system promising for low-temperature NOx removal with ethanol.

Acknowledgments

This work was partially supported by the American Chemical Society Petroleum Research Fund (Grant 41855-AC5) and by the Chemical Sciences, Geosciences and Biosciences Division, Office of Basic Energy Sciences, Office of Science, US Department of Energy (Grant DE-FG02-03ER15457).

References

[1] T.V. Johnson, SAE 2002-01-0285.
[2] M.D. Kass, J.F. Thomas, S.A. Lewis, J.M. Storey, N. Domingo, R.L. Graves, A. Panov, P. Park, SAE 2003-01-3244.
[3] T. Noto, T. Murayama, S. Tosaka, Y. Fujiwara, SAE 2001-01-1935.
[4] S. Sumiya, M. Saito, M. Furuyama, N. Takezawa, K. Yoshida, React. Kinet. Catal. Lett. 64 (1998) 239;
N. Aoyama, S. Sumiya, N. Kakuta, K. Yoshida, React. Kinet. Catal. Lett. 65 (1998) 139;
A. Abe, N. Aoyama, S. Sumiya, N. Kakuta, K. Yoshida, Catal. Lett. 51 (1998) 5.
[5] J.F. Thomas, S.A. Lewis, B.G. Bunting, J.M. Storey, R.L. Graves, P.W. Park, SAE SP-1942, 199.
[6] J.H. Lee, S.J. Schmieg, S.H. Oh, Ind. Eng. Chem. Res. 43 (2004) 6343.
[7] S. Schmieg, B.K. Cho, S.H. Oh, Appl. Catal. B 49 (2004) 113;
T. Miyadera, Appl. Catal. B 13 (1997) 157;
T. Noto, T. Murayama, S. Tosaka, Y. Fujiwara, SAE SP-1626, 45;
S. Kameoka, Y. Ukisu, T. Miyadera, Phys. Chem. Chem. Phys. 2 (2000) 367;
S. Kameoka, T. Chafik, Y. Ukisu, T. Miyadera, Catal. Lett. 51 (1998) 11.
[8] M. Li, Y.H. Yeom, E. Weitz, W.M.H. Sachtler, J. Catal. 235 (2005) 201.
[9] Y.H. Yeom, M. Li, M.H. Sachtler, E. Weitz, J. Catal. 238 (2006) 100.
[10] Q. Wu, H. He, Y. Yu, App. Catal. B 61 (2005) 107.
[11] S. Kameoka, Y. Ukisu, T. Miyadera, Phys. Chem. Chem. Phys. 2 (2000) 367.
[12] N. Bion, J. Saussey, M. Haneda, M. Daturi, J. Catal. 217 (2003) 47.
[13] Y.H. Yeom, B. Wen, W.M.H. Sachtler, E. Weitz, J. Phys. Chem. B 108 (2000) 5386.
[14] G. Fischer, J. Geith, T.M. Klapotke, B. Krumm, Z. Naturforsch. B 57 (2002) 19.
[15] S. Golay, R. Doeper, A. Renken, Appl. Catal. A 172 (1998) 97.
[16] S. Golay, R. Doepper, A. Renken, Chem. Eng. Sci. 54 (1999) 4469.
[17] E.M. Cordi, J.L. Falconer, Catal. Lett. 38 (1996) 45.
[18] NIST Chemistry WebBook, http://webbook.nist.gov.
[19] M.P. Bernstein, S.A. Sandford, L.J. Allamandola, Astrophys. J. 476 (1997) 932.
[20] A. Satsuma, A.D. Cowan, N.W. Cant, D.L. Trimm, J. Catal. 181 (1999) 165.
[21] Y.H. Yeom, J.D. Henao, M. Li, M.H. Sachtler, E. Weitz, J. Catal. 231 (2005) 181.
[22] D.V. Lanzisera, L. Andrews, J. Phys. Chem. A 101 (1997) 9660.
[23] W.-F. Hu, T.-J. He, D.-M. Chen, F.-C. Liu, J. Phys. Chem. A 106 (2002) 7294.
[24] J. Shibata, K.-I. Shimizu, Y. Takada, A. Shichi, H. Yoshida, S. Satokawa, A. Satsuma, T. Hattori, J. Catal. 227 (2004) 367.
[25] A. Satsuma, J. Shibata, K.-I. Shimizu, T. Hattori, Catal. Surv. Asia 9 (2005) 75.
[26] C. Shi, M. Cheng, Z. Qu, X. Bao, J. Mol. Catal. A 235 (2005) 35.
[27] M.D. Baker, G.A. Ozin, J. Godber, J. Phys. Chem. 89 (1985) 305.
[28] P. Sazama, L. Čapek, H. Drobna, Z. Sobalik, J. Dědeček, K. Arve, B. Wichterlová, J. Catal. 232 (2005) 302.
[29] K. Arve, L. Čapek, F. Klingstedt, K. Eränen, E.-E. Lindfords, D.Yu. Murzin, J. Dědeček, Z. Sobalik, B. Wichterlová, Top. Catal. 30 (2004) 91.
[30] K.A. Bethke, H.H. Kung, J. Catal. 172 (1997) 93.
[31] X. She, M. Flytzani-Stephanopoulos, J. Catal. 237 (2006) 79.
[32] P.G. Harrison, E.W. Thorton, J. Chem. Soc. Faraday 1 72 (1976) 2484.
[33] B.A. Morrow, I.A. Cody, J. Chem. Soc. Faraday 1 71 (1975) 1021.
[34] O. Dietz, V.M. Rayon, G. Frenking, Inorg. Chem. 42 (2003) 4977.
[35] G.A. Bowmaker, B.J. Kennedy, J.C. Reid, Inorg. Chem. 37 (1998) 3968.
[36] C.J. Blower, T.D. Smith, J. Chem. Soc. Faraday Trans. 90 (1994) 931.